Research on Engineering Structures & Materials
www.jresm.org
Research Group

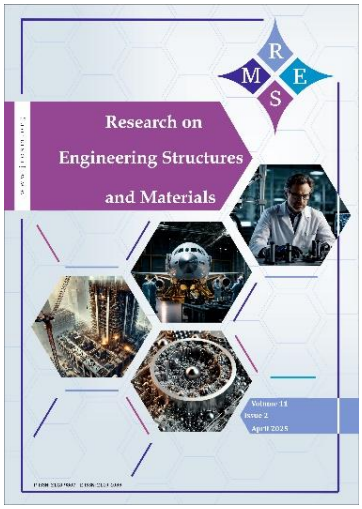

Multi-objective position layout optimization of CNC milling fixture structure integrating remaining useful life prediction model

Qingzhen Zhang, Yanguo Hao

Online Publication Date: 30 August 2026

URL: http://www.jresm.org/archive/resm2026-2074im0730rs.html
DOI: http://dx.doi.org/10.17515/resm2026-2074im0730rs

Journal Abbreviation: *Res. Eng. Struct. Mater.*

To cite this article
Zhang Q, Hao Y. Multi-objective position layout optimization of CNC milling fixture structure integrating remaining useful life prediction model. *Res. Eng. Struct. Mater.*, 2026; 12(5): 3897-3911.

Disclaimer
All the opinions and statements expressed in the papers are on the responsibility of author(s) and are not to be regarded as those of the journal of Research on Engineering Structures and Materials (RESM) organization or related parties. The publishers make no warranty, explicit or implied, or make any representation with respect to the contents of any article will be complete or accurate or up to date. The accuracy of any instructions, equations, or other information should be independently verified. The publisher and related parties shall not be liable for any loss, actions, claims, proceedings, demand or costs or damages whatsoever or howsoever caused arising directly or indirectly in connection with use of the information given in the journal or related means.

Published articles are freely available to users under the terms of Creative Commons Attribution - NonCommercial 4.0 International Public License, as currently displayed at here (the “CC BY - NC”).

Research on Engineering Structures & Materials
www.jresm.org
Research Group

Research Article

Multi-objective position layout optimization of CNC milling fixture structure integrating remaining useful life prediction model

Qingzhen Zhang [*,1,a], Yanguo Hao [2,b]

[1]*Engineering Training Center, Shandong Huayu University of Technology, Dezhou, China*
[2]*School of Mechanical Engineering, Shandong Huayu University of Technology, Dezhou, China*

Article Info

Article History:

Received 30 July 2026

Accepted 20 Aug 2026

Keywords:

CNC tool;
Life prediction;
Multi-objective optimization;
Bidirectional long Short-term memory;
Particle swarm optimization

Abstract

CNC tool accessories are affected by cutting vibration and load impact for a long time, and are prone to fatigue damage. However, traditional optimization methods often ignore the synergy between life and performance, making it difficult to balance service life, structural stiffness, deformation control and other indicators. Therefore, this study proposes a multi-objective topology optimization method that integrates life prediction models. To address the correlation characteristics between vibration signals and life degradation, this study first preprocesses the vibration signals through interpolation method and 3σ criterion. It builds a complete integrated empirical mode decomposition-Fine-to-Coarse signal processing framework with adaptive noise, extracts multi-scale sensitive features, and then designs a CNN-BiLSTM life prediction model. Experiments show that the MAE and RMSE of this model are as low as 0.007 and 0.008, and the average prediction accuracy is 96.1%, which is better than the comparative method. In the test using milling machine fixtures as the object, the proposed multi-objective optimization method of BPNN-PSO converges after 90 iterations, the generation distance is 0.011, the proportion of remaining life after optimization is up to 0.96, and the deformation amount is smaller than other methods. Experimental data demonstrate that the proposed method realizes favorable coordination between precise remaining life prediction and structural performance improvement. Under tested working conditions, this approach attains a satisfactory trade-off between fixture service life and deformation control, offering an effective technical reference for the design of CNC tool attachments.

© 2026 MIM Research Group. All rights reserved.

1. Background

In the context of the transformation of modern manufacturing to high precision, high efficiency, and high reliability, CNC tools are core processing equipment, and the performance of their accessory structures (especially fixtures) directly determines processing accuracy, production efficiency, and operational safety. During long-term service, fixtures are easily affected by complex working conditions such as cutting vibration and load impact, and are prone to fatigue damage and performance degradation. This not only shortens their service life but may also increase workpiece machining errors or cause safety accidents [1,2]. Therefore, how to achieve collaborative optimization of life and performance during the structural design stage has become a key technical problem in the research and development of CNC tool accessories. At present, the structural optimization of CNC tool accessories mostly focuses on improving mechanical properties, often ignoring the correlation between life prediction and optimal design, making it difficult for the optimization plan to take into account core indicators such as service life, structural stiffness, and

*Corresponding author: zhangqingzhen136@163.com
[a]orcid.org/ 0009-0008-5522-979X; [b]orcid.org/ 0009-0000-8046-5841
DOI: http://dx.doi.org/10.17515/resm2026-2074im0730rs

deformation control. Meanwhile, traditional life prediction methods rely on empirical models or single signal features, which are difficult to effectively capture the multi-scale sensitive information related to life degradation in vibration signals, and the prediction accuracy is insufficient [3,4]. Existing structural optimization algorithms often have problems such as slow convergence speed and easy falling into local optima, making it difficult to efficiently solve Multi-Objective Optimization (MOO) problems. In response to the above challenges, there is an urgent need to establish a Multi-Objective Position Layout Optimization (MPLO) framework that integrates accurate life prediction.

Bidirectional Long Short-Term Memory (BiLSTM) enhances the model's ability to understand sequence data by simultaneously processing past and future information at each time step. Duan et al. proposed a parallel BiLSTM MHA prediction framework that integrates multi head attention mechanism to address the issue of insufficient accuracy in predicting the remaining service life of lithium-ion batteries. This framework first constructs multidimensional features of the battery's entire lifecycle to complete capacity estimation, and then combines the CEEMDAN module to achieve remaining life prediction based on the estimated capacity, fully mining the multidimensional temporal information of the battery and taking into account the capacity regeneration effect. Based on the NASA and CALCE battery datasets, case validation was conducted, and the results showed that this method has better performance in predicting the remaining service life of lithium-ion batteries compared to traditional deep learning models [5]. Zhang et al. proposed the VMD-CNN BiLSTM prediction model to address the issue of low accuracy in traditional methods for predicting the remaining life of turbofan engines under variable operating conditions. This method first processes data through variational mode decomposition to extract multidimensional temporal features and eliminate abnormal samples. Then, CNN is used to complete feature mapping and BiLSTM is combined to mine temporal dependencies. At the same time, sparrow algorithm is introduced to optimize model hyperparameters and improve prediction performance. Based on the C-MAPSS dataset, experiments were conducted and the results showed that the model predicted a root mean square error of 13.74 ± 0.51 and an average absolute error of 11.24 ± 0.49, demonstrating excellent prediction accuracy and generalization ability even in noisy data [6]. Yuan et al. proposed an integrated life prediction framework that combines an improved whale optimization algorithm with adaptive variational mode decomposition and CNN BiLSTM predictor to address the problem of difficulty in achieving reliable signal decomposition and accurate mapping of health indicators to life for predicting the remaining service life of rolling bearings. This framework utilizes IWOA and entropy guided objective function to optimize VMD parameters, screen effective intrinsic modal components, and construct a lightweight self-attention health index SA-HI to characterize the degradation trend of bearings. Based on the XJTU-SY bearing dataset, multiple experiments were conducted, and the results showed that SA-HI had better monotonicity, trendiness, and robustness than traditional indicators. The entire framework was able to achieve more accurate and stable remaining life prediction in both same and cross condition tests, and its performance was superior to mainstream deep learning comparison models [7].

Particle Swarm Optimization (PSO) algorithm can simulate the foraging behavior of flocks of birds and fish. The core idea is to find the optima in the solution space through the collaboration and information sharing of individuals in the group. Hrechanyi explores the method of determining equipment detection intervals based on non-stationary Poisson flow emission theory for predicting the timing of maintenance start-up of metallurgical equipment during degradation processes. The research focuses on analyzing the process of equipment degradation, using emission theory to plan periodic detection cycles, and completing parameter determination by comparing paired correlation coefficients, requiring the correlation coefficient to approach 1. The research results show that when using the emission theory to allocate equipment mutual control cycles, a correlation coefficient close to 1 should be used as the criterion for discrimination, in order to support the construction of detection interval planning algorithms [8]. The Backpropagation Neural Network (BPNN) inverse system decoupling control of the permanent magnet-assisted bearingless synchronous reluctance motor has problems such as slow convergence, easy falling into local optimum, low fitting accuracy and poor generalization ability. Liu et al. proposed a full-speed domain dynamic decoupling control strategy based on enhanced chaotic PSO. The dynamic

decoupling performance between velocity, x- and y-direction radial displacement has been improved, and the static stability and dynamic responsiveness of the system have verified the effectiveness of this scheme [9]. Lin and Sheu proposed an optimization method combining PSO and Simulated Annealing (SA) algorithms for the magnetic delay optimization problem of Fe3O4 ferrofluid coating. This method conducted experiments through the uniform design method, used stepwise regression analysis to make the formula consistent with the experimental data, and then used two intelligent search methods, PSO and SA, to find the maximum delay. The optimized parameter combination could significantly improve the magnetic delay [10].

To sum up, existing research on the intrinsic relationship between multi-segment life prediction and structural design makes it difficult to take into account indicators such as service life, stiffness, and deformation control. Moreover, single signal processing is difficult to fully exploit the multi-scale sensitive features of vibration data, traditional prediction models are insufficiently accurate, and conventional optimization algorithms are prone to falling into local optima. Given this, this study combines BiLSTM and PSO to propose a CNC tool accessory structure MPLO method that integrates life prediction models to enhance the structural performance of CNC tool accessories while ensuring its service life. The innovation points are: first, a signal processing method grounded on Complete Ensemble Empirical Mode Decomposition with Adaptive Noise (CEEMDAN) and Fine-to-Coarse (FTC) is proposed, and fused with Convolutional Neural Network (CNN) and BiLSTM for life prediction. Secondly, a Fixture Positioning Layout (FPL) optimization model is constructed with the objectives of minimum maximum deformation, minimum overall deformation, and maximum service life. BPNN is used to accurately map the layout and deformation relationship, integrate the life prediction into the fitness function of the PSO algorithm, and adopt the ideas of Dynamic Inertia Weight (DIW) and Pareto Optimal Solution (POS) to achieve collaborative optimization of performance and life, avoiding traditional optimization that ignores the life problem.

2. Research Design

2.1 Structural Life Prediction Method of CNC Tool Accessories Based on CNN-BiLSTM

CNC tool accessories (the core is the fixture) are subjected to alternating loads and vibration impacts for a long time during cutting processing, and their life degradation process is highly related to the timing characteristics of the vibration signal. Accurately capturing this correlation is the core prerequisite for structural life prediction. Before optimizing the structure of CNC tool attachments, its lifespan needs to be predicted first. By accurately predicting the remaining life of a structure, key data support can be provided for structural optimization, helping to design more efficient, safer, and more economical structures. Vibration is a primary factor causing fixture damage, which induces fatigue crack initiation and aggravates wear. As the core stress-bearing component of CNC tool accessories, the amplitude and frequency changes of its vibration signal directly reflect the initiation and expansion process of fatigue damage, and are a key data source for life prediction. Therefore, this study constructs a vibration signal processing method that integrates CEEMDAN and FTC. First, the vibration signal needs to be preprocessed. For the problem of missing vibration signals, this study uses the interpolation method to approximately supplement the missing values, so that the signal fluctuation tends to normal. For outliers, this study uses the 3σ criterion for detection and processing through manual deletion or interpolation. The above preprocessing operation can effectively eliminate irrelevant noises such as electromagnetic interference and equipment start-stop impact in the cutting environment, retain effective vibration information directly related to fixture life degradation, and provide guarantee for the accuracy of subsequent feature extraction. After preprocessing the vibration signal, it can be decomposed by CEEMDAN to obtain six intrinsic mode function (IMF) components. Among them, IMF1 has the highest frequency and decreases in sequence. The high-frequency IMF component mainly corresponds to the instantaneous impact vibration during the cutting process, and is directly related to the fixture surface wear and micro-crack expansion. The low-frequency IMF component reflects the overall vibration characteristics of the structure and is related to the fatigue degradation trend of the fixture matrix. By analyzing the mean value of the IMF components, vibration characteristics can be revealed. After decomposing the signal, the FTC algorithm can be

used to extract its features. This method first screens high- and low-frequency IMFs, then constructs a pool of them, then calculates the fusion weight, and finally fuses and reconstructs the IMF components. Through these steps, the sensitive features in the IMFs component data can be fully obtained. The instantaneous impact load during milling processing will cause the local stress of the fixture to instantly exceed the yield limit of the material, resulting in plastic strain accumulation. A single overload will form micro defects on the surface of the component, and under multiple impacts, micro cracks will continue to propagate along the stress concentration points; Under the coupling effect of alternating vibration and overload, damage accumulates nonlinearly, and the damage rate increases exponentially with the peak load. From a mathematical perspective, the Miner linear damage accumulation criterion can be used to quantify the incremental damage caused by a single impact, which is positively correlated with the load amplitude and duration. When the total damage accumulates to a critical value, the fixture experiences fatigue failure, and this mechanism is also the core cause of high-frequency components in vibration signals [11]. The energy calculation of the IMF component is shown in Equation (1).

$$E_i = \int |IMF_i(t)|^2 dt = \sum_{j=1}^{J} \left|x_{ij}^2\right| \tag{1}$$

In Equation (1), E_i means the energy of the i-th IMF component. $IMF_i(t)$ is the i-th IMF component at time t. J is the number of IMF component data points. x_{ij} is the amplitude of each point in the IMF component. At this time, the calculation of the total energy of IMF E is shown in Equation (2).

$$E = \sum_{i=1}^{n} E_i \tag{2}$$

Since IMF components with small amplitude energy will be overwhelmed by IMF components with large amplitude energy, to avoid the above problems, the IMF energy also needs to be normalized to obtain weights. The weight formula is Equation (3).

$$\omega_i = \frac{E_i}{E} \tag{3}$$

In Equation (3), ω_i is the weight. The relationship between weight and IMF energy is shown in Equation (4).

$$\omega_1 : \omega_2 : \cdots : \omega_k = E_1 : E_2 : \cdots : E_k \tag{4}$$

In Equation (4), the weight is proportional to the IMF energy. At this time, the IMF component fusion result is defined as Equation (5).

$$F(t) = \omega_1 IMF_1 + \omega_2 IMF_2 \ldots + \omega_k IMF_k \tag{5}$$

In Equation (5), $F(t)$ is the IMF component fusion result. Finally, the vibration signal characteristics can be obtained by reconstructing the features using the phase space reconstruction method. After extracting the vibration signal features, CNN-BiLSTM can be used to predict the structural life of CNC tool accessories. In view of the nonlinear and long-term characteristics of the life degradation of CNC tool attachment fixtures, the CNN module can effectively extract local key information in the vibration characteristics. The BiLSTM module can deeply mine long-term dependencies in feature sequences and accurately capture the gradual law of life decay. The structure of CNN-BiLSTM is shown in Fig.1.

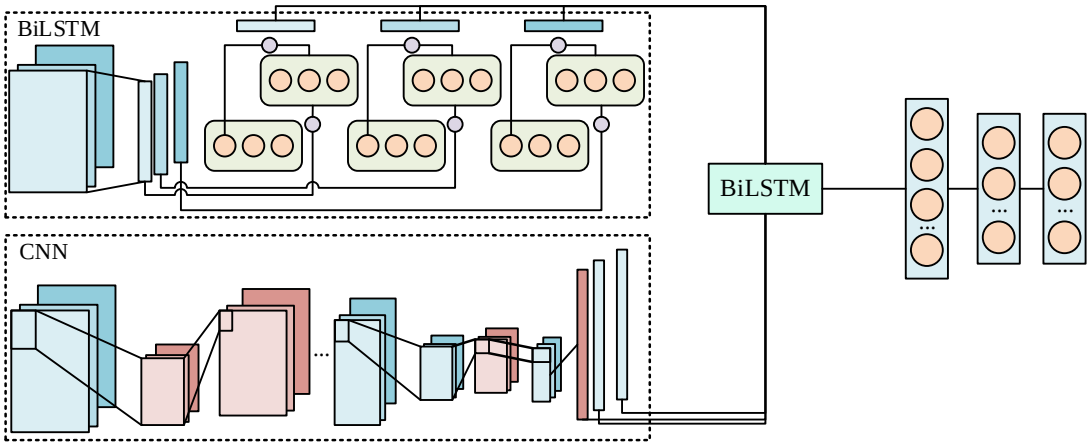

Fig. 1. Framework of CNN-BiLSTM

In Fig.1, the model adopts a dual-branch structure: CNN extracts the lifetime degradation characteristics of low-frequency data, and BiLSTM extracts the lifetime degradation characteristics of high-frequency data. After the features are fused, the Fully Connected Layer (FCL) predicts the remaining service life. The model architecture is specifically adapted to the complex characteristics of the fixture vibration signal. The collaborative design of the dropout layer and the FCL can effectively avoid prediction overfitting caused by fluctuations in cutting conditions, ensuring that the remaining life prediction results of the fixture can be stably output under different processing loads. Fig.2 shows the framework of the designed CNN model.

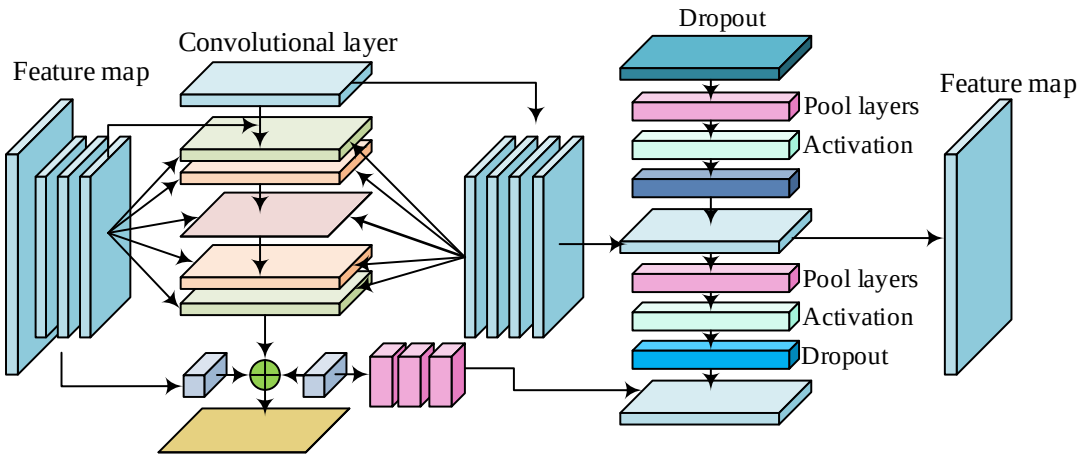

Fig. 2. Structure of CNN

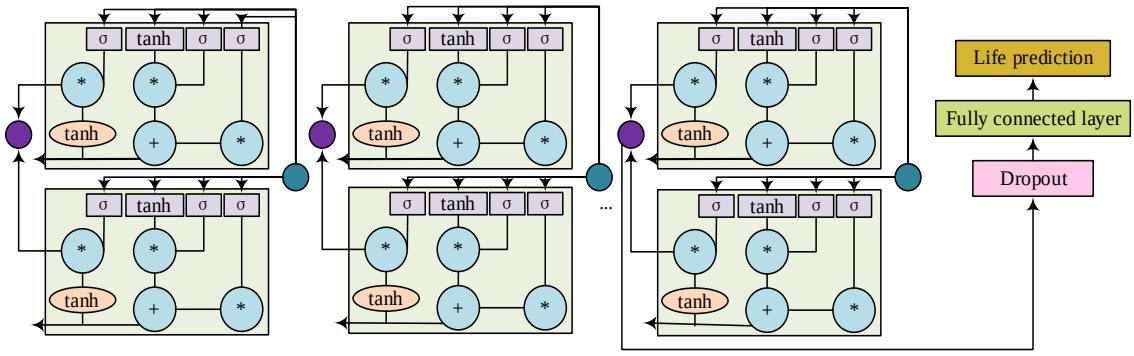

Fig. 3. Structure of BiLSTM

In Fig.2, the constructed deep CNN model contains a total of 4 convolutional blocks in series. Each convolutional block uses a 1D convolutional layer as the core computing unit, equipped with a ReLU activation function for nonlinear transformation, followed by a 1D maximum pooling layer for

downsampling. To balance feature extraction capability with sequence length preservation, the first and fourth convolutional blocks retain pooling operations to compress the data dimension and enlarge the receptive field. The second and third convolutional blocks deliberately remove the maximum pooling layer, and only extract local deep features through the convolutional layer to avoid the loss of key timing information caused by excessive downsampling, thereby more precisely capturing the pattern features in the signal [12]. The structure of BiLSTM is shown in Fig.3.

In Fig.3, the structure includes an input layer (IL), a BiLSTM layer, an FCL, and an output layer (OL). Among them, the number of neurons in the 1st and 2nd BiLSTM layers is 300 and 150, the number of neurons in the FCL is 128, the activation function is ReLU, and the Dropout ratio is 0.5. For the number of predicted branches, this study uses the grid search method to determine [13-15]. For the prediction results of each branch, this study uses a weighted voting method to integrate them. The voting weight is calculated as shown in Equation (6).

$$w_i^j = \frac{P_i^j}{\sum_{k=1}^{s} P_{r_i}^s} \tag{6}$$

In Equation (6), w_i^j and P_i^j are the weight and prediction percentage of test sample i in prediction branch j. The final prediction results are shown in Equation (7).

$$R = w_i^1 R_i^1 + w_i^2 R_i^2 + \cdots + w_i^k R_i^k \tag{7}$$

In Equation (7), R and R_i^k are the prediction results of the final and branch paths. Through the above method, the structural life of CNC tool accessories can be accurately predicted.

2.2 CNC Tool Attachment Structure Optimization Method Based on BPNN-PSO

After life prediction is performed through CNN-BiLSTM, the CNC tool attachment structure can be optimized based on the prediction results. As an important accessory structure of CNC tools, the performance of the fixture has a crucial impact on production efficiency and product quality. FPL plays a vital role in mechanical processing. It not only directly affects the processing accuracy, efficiency and final quality of the workpiece, but also has a significant impact on the service life of the fixture. Therefore, to improve the processing quality and service life, this study proposes the FPL-MOO method based on BPNN-PSO. The FPL-MOO model is Equation (8).

$$\begin{cases} Findx = [x_1, x_2, \cdots, x_N, \alpha_1, \alpha_2, \cdots, \alpha_N] \\ min\, f_1(x) = max\{|u_i(x)|\} \\ min\, f_2(x) = \sqrt{\frac{\sum_{i=1}^{K} u_i{}^2(x)}{K}} \\ max\, f_3 = L(x) \\ s.t. x_i \in \Omega, x_j \in \Omega and x_i \neq x_j, \alpha_i \in \Gamma \end{cases} \tag{8}$$

In Equation (8), x is the design variable. x_i is the coordinates of the anchor point. α_i is the contact characteristic parameter of the positioning point. $f_1(x)$, $f_2(x)$, and $f_3(x)$ are the maximum deformation, overall deformation and service life. u_i is the Z-direction displacement of the node. K is the number of nodes. $L(x)$ is the remaining service life. Ω is the set of feasible regions. Γ is the feasible region of contact parameters. The candidate fixture layout design variable x is input into finite element simulation to obtain vibration timing signals, which are preprocessed by CEEMDAN-FTC to extract multi-scale features and fed into the trained CNN BiLSTM life prediction model to output the $L(x)$ corresponding to the layout. Complete calculation chain: layout parameters → simulated vibration data → feature extraction → CNN BiLSTM inference → $L(x)$. Construct a PSO fitness function by combining the remaining service life with the maximum and

overall deformation, to achieve quantitative solution of fitness for each generation of particles and ensure algorithm reproducibility. The objective function of minimizing the maximum and overall strain in this article is directly related to the flow stress of the fixture material: the lower the yield flow stress of the material, the more significant the plastic deformation under the same clamping load. Simultaneously milling the thermo mechanical coupling stress will intensify strain accumulation, and the cutting temperature and feed rate in the machining process will change the instantaneous stress field of the component. As a core structural factor, the positioning layout can change the stress concentration area. Reasonable arrangement of positioning points can disperse the thermal mechanical composite load, reduce local stress peaks, suppress plastic deformation beyond flow stress, and achieve strain index optimization [16,17]. To optimize FPL, this study adopts the POS idea, generates samples through uniform experimental design method, establishes a BPNN model, and maps the relationship between FPL and thin plate deformation. Finally, MOO is performed to get POS. The optimization process based on BPNN-PSO is shown in Fig.4.

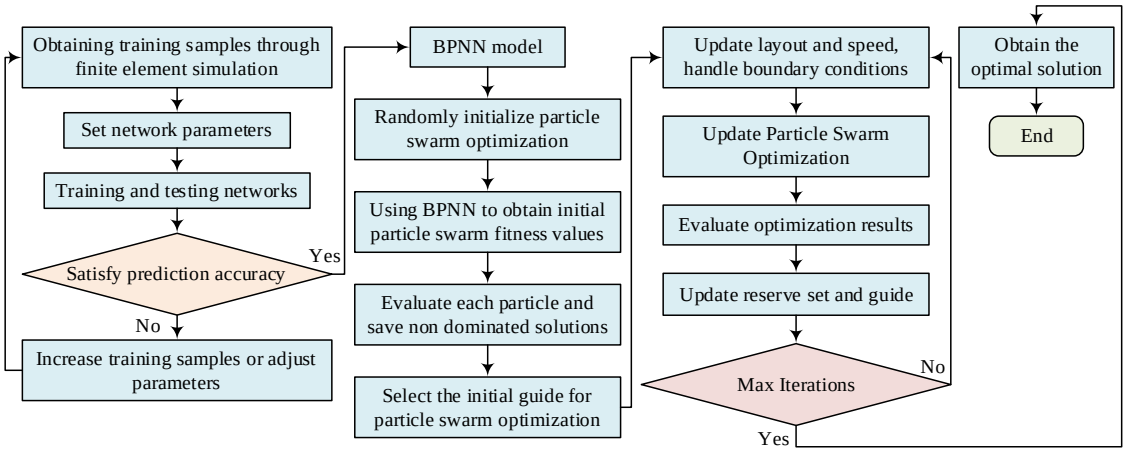

Fig. 4. Optimization process based on BPNN-PSO

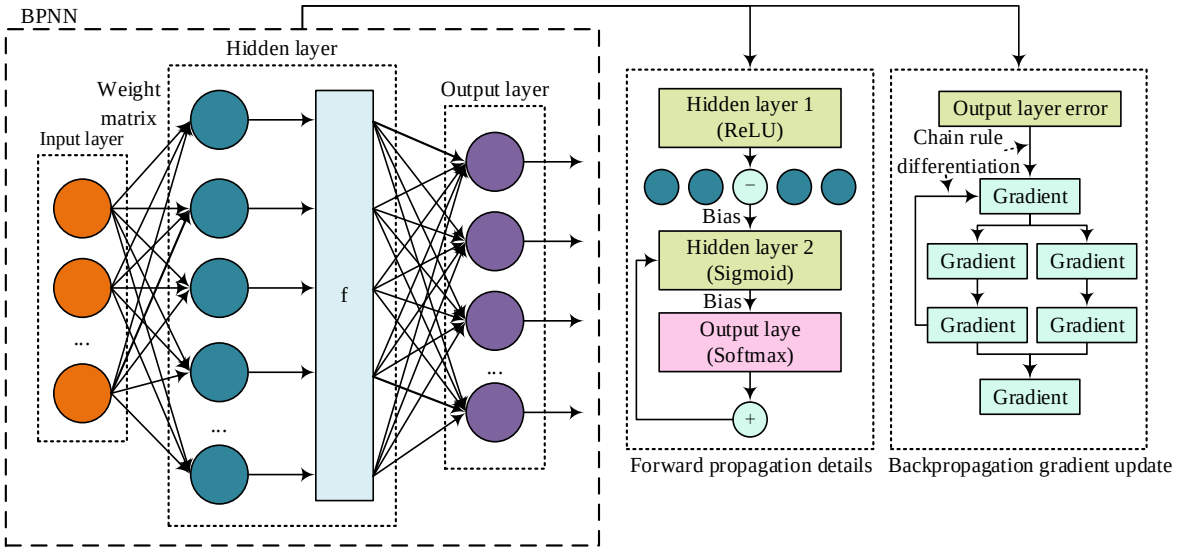

Fig. 5. Structure of BPNN

In Fig.4, first, the layout samples are uniformly selected within the positioning constraint range, and the deformation data is obtained through finite element simulation, and a three-layer BPNN prediction model is constructed at the same time. The network parameters are adjusted by comparing the prediction errors, the positioning layout is encoded, the initial particle swarm is generated, and BPNN is used to evaluate the fitness. By optimizing the solution set through the Pareto dominance relationship and the GD evaluation index, the optimal positioning point coordinate solution set and the corresponding deformation are obtained. The fixture material for

the finite element model is 45 steels, with an elastic modulus of 210GPa and a Poisson's ratio of 0.3; Adopting a solid hexahedral structured grid and encrypting the grid in key positioning areas. Boundary conditions: The fixture base is fully fixed with constraints, and milling equivalent alternating cutting loads are applied to each positioning point. After completing the grid independence verification, batch simulation is conducted to extract the Z-direction displacement of nodes under each layout, calculate the maximum deformation and overall deformation mean, and use them as input sample data for the BPNN network. The structure of BPNN is shown in Fig.5.

In Fig.5, BPNN includes an IL, one or more hidden layers, and an OL. Each node (neuron) in the network is connected by weights and contains an activation function to introduce nonlinearity. The IL receives data, the hidden layer processes and extracts features, and the OL generates prediction results. Since the performance of BPNN is affected by the number of hidden layers and nodes, too much will take more time. Therefore, this study uses two layers of hidden layers and determines the number of nodes through a trial-and-error method [18]. The number of IL nodes of the model is the number of parameters that affect the fixture layout, and the number of OL nodes is determined based on the prediction target. At the same time, this study reduces the prediction error to the target value by adjusting the weights, and builds a multi-objective neural network based on the sim function of the MATLAB toolbox. The expression of the number of hidden layer nodes h is shown in Equation (9).

$$h = \sqrt{l + m} + c \tag{9}$$

In Equation (9), l means the number of neurons in the IL. m denotes the number of output nodes. c is a positive integer. Then, the PSO algorithm can be used to implement the fixture layout. The MOO process based on PSO is shown in Fig.6.

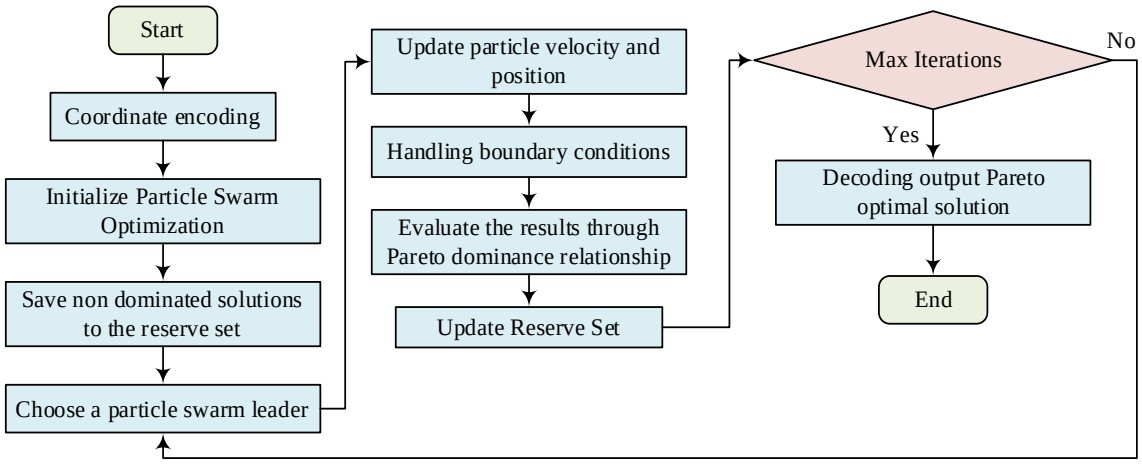

Fig. 6. MOO process based on PSO

In Fig.6, the optimization variables such as the fixture positioning coordinates are first encoded in real numbers, the search boundary and population size are preset, and the particle parameters are randomly initialized. Then, based on multi-objective functions such as clamping error and stability, individual fitness is calculated. The Pareto dominance relationship is used to filter non-dominated solutions to construct elite files, and the particle speed and position are updated accordingly. If a boundary violation occurs during the iteration, the boundary absorption strategy can be used to limit the particles to the feasible region to ensure the convergence of the optimization process and the validity of the solution [19,20]. The iterations are repeated until convergence, and the POS set is obtained, which is the optimal solution of FPL. The speed update formula of PSO is shown in Equation (10).

$$s_i(t+1) = \beta s_i(t) + m_1 r_1(t)(v_{si}(t) - x_i(t)) + m_2 r_2(t)\left(v_{gi}(t) - x_i(t)\right) \tag{10}$$

In Equation (10), $s_i(t+1)$ is the particle speed when iterating $t+1$ times. β is the inertia weight coefficient. m_1 and m_2 are acceleration constants. Both r_1 and r_2 are random numbers. $x_i(t)$ is the particle position at $t+1$ iterations. v_{si} and v_{gi} are individual optimal values and global optimal values. The position update formula is shown in Equation (11).

$$x_i(t+1) = x_i(t) + s_i(t+1) \tag{11}$$

Since the inertial weight has a significant impact on the particle speed, to avoid falling into a local optimum and ensure the convergence speed, this study uses DIW. Equation (12) is the inertia weight formula.

$$\beta = \beta_{\max} - \frac{(\beta_{\max} - \beta_{\min})t}{T_{\max}} \tag{12}$$

In Equation (12), $\beta_{\max}$ and $\beta_{\min}$ are the maximum and minimum inertial weights. $T_{\max}$ means the maximum iterations. For the convergence of the optimal solution set, this study uses generation distance to evaluate. Equation (13) is the generation distance formula.

$$D = \left(\frac{1}{n} \sum_{i=1}^{n} d_i^p \right)^{1/p} \tag{13}$$

In Equation (13), D is the generation distance. n is the number of Pareto front solutions. d_i is the Euclidean distance between individual i and the closest individual to the real Pareto front. p takes the value 2. MOO for FPL can be achieved through the above method.

3. Results

3.1 Analysis of Life Prediction Results

To verify the proposed life prediction model, this study tests and compares it with Wasserstein Generative Adversarial Network-LSTM (WGAN-LSTM) and Residual Convolutional Block Attention Time Convolutional Network-Vision Transformer (RCATCN-ViT). The experimental dataset is CMAPSS, which contains four subsets, with a total of 709 training samples and a total of 707 test samples. The CMAPSS dataset contains 4 sets of aircraft engine timing samples, recording degradation monitoring signals such as temperature, pressure, and vibration throughout the entire lifecycle. It includes 709 sets of training samples and 707 sets of testing samples. The validation of the life prediction model was completed using the CMAPSS dataset for aircraft engines, both of which belong to mechanical degradation objects under cyclic alternating loads, and the degradation mechanisms have commonalities. The degradation mode of fatigue peeling and performance degradation of aviation turbine blades is highly consistent with the evolution law of fatigue cracks and surface wear caused by long-term cutting vibration and impact loads on milling machine fixtures. Time series signals that characterize performance degradation, such as turbine speed and exhaust temperature, can be compared to the vibration amplitude and frequency characteristics of fixtures; The trend of capacity attenuation throughout the entire lifecycle of the turbine corresponds to the degradation curve of the remaining life of the fixture. The prediction model trained on this dataset can be transferred and adapted to the task of predicting the life of fixture vibration signals. In the experiment, the learning rate and batch size are 0.0001 and 128, and the regularization parameter and maximum number of iterations are 1.2 and 200. To determine the optimal number of predicted branches, this study first analyzes the prediction results of different branch numbers. Experimental procedure: 1 Data preprocessing: interpolation to complete missing values, 3 σ criterion to remove outliers, CEEMDAN decomposition of signals, FTC fusion of sensitive IMF components; 2. Model input: Normalize fusion features and divide fixed length sample sequences in chronological order; 3. Training process: Learning rate of 0.0001, batch size of 128, 200 iterations, using 10 branch weighted voting to output lifetime results, Dropout=0.5 to suppress overfitting, fixed random seeds throughout the process to ensure reproducibility of the

experiment. Prediction accuracy: Based on the true remaining lifespan, if the single sample error is within the allowable threshold, the prediction is considered valid. The proportion of valid samples to the total sample is the accuracy. Score is a specialized evaluation index for life prediction, and the larger the error, the more points will be deducted. The calculation formula is constructed based on the relative deviation between the predicted value and the true value; The higher the values of the two, the better the prediction performance. Table 1 is a comparison of predictions for different branch numbers.

In Table 1, as the Number of Predicted Branches (NoPB) increases, both MAE and RMSE first decrease and then increase. When NoPB is 10, both MAE and RMSE reach the minimum, which are 0.007 and 0.008. This shows that the optimal NoPB is 10. The comparison of remaining life predictions of different methods is shown in Fig.7.

Table 1. Prediction results for different numbers of branches

Number of branches	MAE	RMSE
3	0.043	0.045
4	0.037	0.040
5	0.031	0.032
6	0.025	0.025
7	0.013	0.017
8	0.012	0.013
9	0.008	0.011
10	0.007	0.008
11	0.010	0.013
12	0.010	0.014

Note: MAE Mean Absolute Error; RMSE Root Mean Square Error.

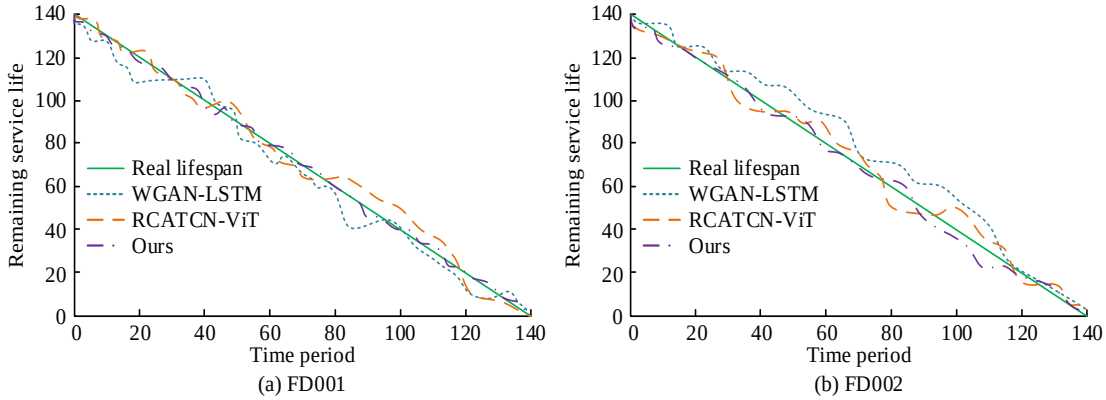

Fig. 7. Remaining life prediction results of different methods

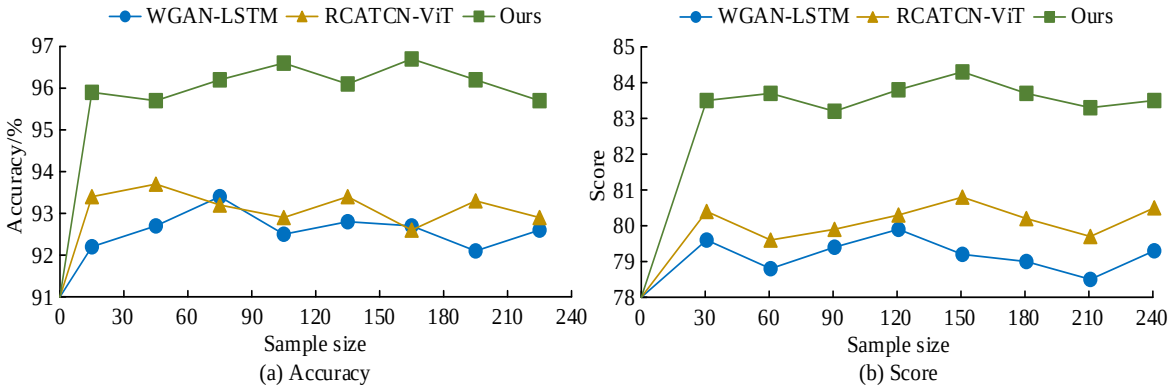

Fig. 8. Prediction accuracy and Score of different methods

In Fig.7(a), for the FD001 subset, the remaining life prediction curves of WGAN-LSTM and RCATCN-ViT fluctuate significantly, and the fit with the real life is poor. The curve of the research method

fluctuates less and basically fits the real-life span. In Fig.7(b), in the FD001 subset, compared with WGAN-LSTM and RCATCN-ViT, the curve of the research method also fluctuates less and has a higher degree of fit with the real-life span. This shows that the research method can achieve accurate prediction of remaining life. The prediction accuracy and Score of different methods are shown in Fig.8.

In Fig.8(a), the lifespan prediction accuracy of WGAN-LSTM and RCATCN-ViT is the highest at 93.4% and 93.7%, and the average accuracy is 92.6% and 93.2%. The highest prediction accuracy of the research method is 96.7%, and the average accuracy is 96.1%, which is higher than other methods. In Fig.8(b), the highest Scores of WGAN-LSTM and RCATCN-ViT are 79.9 and 80.8, and the average Scores are 79.2 and 80.2. The highest Score of the research method is 84.3, and the average Score is 83.6, which is also higher than the comparative methods. Therefore, the life prediction accuracy of the research method is higher. The comparison of predictive performance with integrated machine learning is shown in Table 2.

Table 2. Prediction performance comparison with ensemble machine learning

Model	MAE	RMSE
Random Forest (RF)	0.034	0.036
XGBoost	0.021	0.023
LightGBM	0.018	0.020
Proposed CNN-BiLSTM	0.007	0.008

According to Table 2, the MAE and RMSE of these three ensemble algorithms are significantly higher than those of the CNN BiLSTM framework. Thanks to the multi-scale feature fusion of CEEMDAN-FTC and the dual branch deep network architecture, this method can automatically mine long-term fatigue degradation rules, providing more accurate remaining life prediction for CNC tool accessories. To further explore the performance of the proposed method, this study conducts an ablation experiment on it, as listed in Table 3.

Table 3. Results of experiment

Model	CEEMDAN	FTC	CNN	RMSE
1	×	×	×	0.059
2	√	×	×	0.042
3	×	√	×	0.040
4	×	×	√	0.037
5	√	√	×	0.031
6	√	×	√	0.025
7	×	√	√	0.016
8	√	√	√	0.008

In Table 3, after introducing each module, the RMSE of the model is significantly reduced. CNN has the most significant impact on model performance. After introducing this module, the RMSE of the model drops by 37.3%. This shows that the improved method can effectively improve the life prediction accuracy of CNC tool attachment structures.

3.2 Analysis of Optimization Results of CNC Tool Attachment Structure

To verify the performance of the optimization method, this study tests it and compares it with the Multi-objective Gray Wolf Optimization Algorithm - Radial Basis Function (MOGWO-RBF) and the Improved PPSO-SA Algorithm (IPSO-SA). This study takes the fixture of a CNC milling machine as an example to test it. The iteration curves and POS sets of different methods are shown in Fig.9.

In Fig.9(a), compared with MOGWO-RBF and IPSO-SA, the research method has better convergence and converges after 90 iterations. Its generation distance is only 0.011, which is lower than other methods. In Fig.9(b), the Pareto optimal overall deformation and maximum deformation of the research method are smaller. Therefore, the optimization results of the research method are better. Table 4 shows the fixture layout optimization results under different weights.

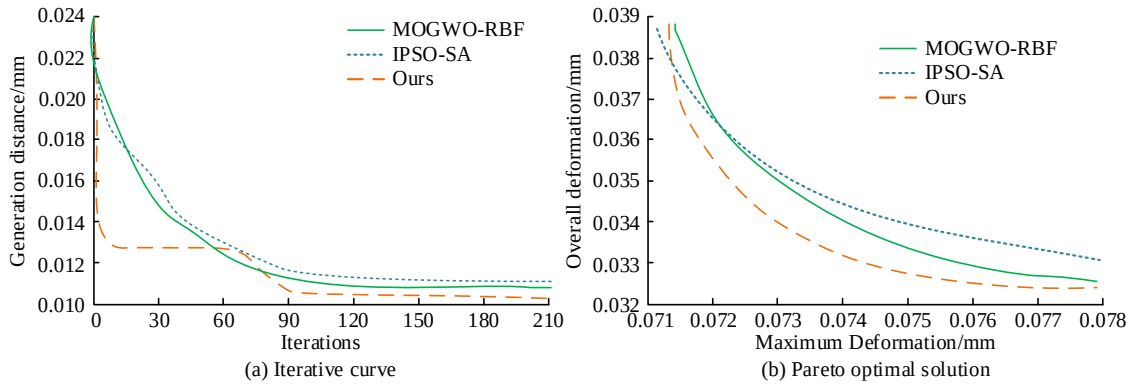

Fig. 9. Iterative curves and POS set for different methods

Table 4. Optimization results of fixture layout under different weights

Anchor point	Weight	MOGWO-RBF	IPSO-SA	Ours
1	0.5	(362.74,235.89)	(356.84,230.92)	(358.94,232.93)
	1.0	(360.22,232.51)	(356.15,234.34)	(358.17,235.47)
2	0.5	(166.38,341.20)	(165.18,337.27)	(164.53,338.18)
	1.0	(169.25,337.53)	(166.73,337.55)	(167.07,338.94)
3	0.5	(63.21,143.74)	(60.12,143.86)	(61.82,144.53)
	1.0	(63.05,148.16)	(62.76,148.97)	(61.06,147.07)
4	0.5	(257.24,43.56)	(257.11,42.36)	(255.47,41.82)
	1.0	(254.67,42.95)	(253.97,40.85)	(252.93,41.06)
Proportion of remaining lifespan	0.5	0.88	0.83	0.96
	1.0	0.84	0.78	0.93

In Table 4, compared with other methods, the layout optimization results of the research method have a larger proportion of remaining life. Taking a weight of 0.5 as an example, the remaining life proportions of MOGWO-RBF, IPSO-SA, and research methods are 0.88, 0.83, and 0.96. The research method can effectively balance the remaining life and performance of the structure when optimizing the CNC tool attachment structure.

4. Discussion and Interpretation

This paper focuses on the life prediction and MPLO of CNC tool attachment structures. By constructing an integrated method that integrates signal processing, DL, and intelligent optimization, it achieves a dual improvement in prediction accuracy and optimization performance. Relevant experimental data provide sufficient support for the effectiveness of the method. In life prediction experiments, the choice of NoPB has a significant impact on model performance. As NoPB increases from 3 to 10, MAE and RMSE continue to decrease and reach the minimum values (0.007, 0.008), while the error increases after NoPB exceeds 10. This shows that the weighted voting mechanism of 10 prediction branches can optimally integrate multi-dimensional degradation features and avoid the prediction deviation of a single branch and redundant calculations caused by too many branches. Compared with WGAN-LSTM and RCATCN-ViT, CNN-BiLSTM performs better in remaining life fitting, prediction accuracy, and Score indicators: The average prediction accuracy reaches 96.1%, which is 3.5% and 2.9% higher than the comparative method; The average Score is 83.6, which is 3.4~4.4 higher than the comparative method, verifying the model's capacity to capture long-term degradation patterns.

In the CNC tool attachment structure optimization experiment, with milling machines as the research object, the BPNN-PSO method is superior to MOGWO-RBF and IPSO-SA in terms of convergence and optimization effects. This method reaches stable convergence after 90 iterations, and the generation distance is only 0.011, which is lower than the comparison algorithm, indicating that the combination of DIW and POS ideas effectively balances global search and local convergence

efficiency. The optimization results show that under different weight settings, the FPL optimized by the research method can achieve smaller overall deformation and maximum deformation, and the proportion of remaining life is significantly increased: When the weight is 0.5, the proportion of remaining life reaches 0.96, which is 8.9% and 15.7% higher than that of MOGWO-RBF (0.88) and IPSO-SA (0.83). When the weight is 1.0, the proportion of remaining life still maintains a high level of 0.93, proving that this method can achieve the optimal balance between structural performance and service life. This result benefits from BPNN's accurate mapping of the relationship between positioning layout and deformation, and the efficient solution of the MOO problem by the PSO algorithm, which offers a quantitative basis for the engineering design of FPL.

Comparing this article's CNN BiLSTM with traditional probabilistic life prediction methods, the probabilistic model relies heavily on fixed degradation distribution assumptions and is difficult to adapt to complex coupled vibration conditions of fixtures, resulting in poor generalization. And the machine learning method in this article does not require a pre-set degradation model and can adaptively mine multi-scale sensitive vibration features; Paired with BPNN-PSO multi-objective optimization, it can simultaneously consider multiple indicators such as lifespan, stiffness, and deformation. Experiments have shown that compared to probabilistic methods such as Gaussian processes and Wiener processes, this approach has lower prediction errors, faster optimization convergence speed, and is more suitable for the collaborative design requirements of CNC accessories under multiple working conditions.

In summary, the proposed structural optimization method for CNC tool accessories can effectively improve the mechanical properties and service life of the structure. However, this study still has certain limitations, that is, the optimization process does not fully consider the constraints of processing costs and assembly processes. In the future, it should be considered to incorporate indicators such as economic cost and process feasibility into the optimization goals at the same time to build a MOO model that is more in line with engineering reality.

4. Summary

Aiming at the prominent contradiction that traditional structural topology optimization of CNC tool attachments ignores the coupling relationship between fatigue life and mechanical performance, this study constructs an integrated multi-objective topology optimization framework embedded with high-precision remaining useful life prediction model, and systematically verifies the effectiveness and superiority of the whole technical route through signal processing experiments, deep learning comparative tests and multi-objective optimization engineering cases. In the life prediction module, this paper combines CEEMDAN signal decomposition and FTC multi-scale sensitive feature fusion to fully mine degradation information hidden in cutting vibration signals, and builds a dual-branch CNN-BiLSTM prediction model with weighted multi-branch voting strategy. Grid search experiments confirm that setting 10 prediction branches can achieve optimal prediction accuracy, where the model's MAE and RMSE reach ultra-low values of 0.007 and 0.008 respectively, with an average prediction accuracy up to 96.1%. Ablation experiments further prove that CEEMDAN, FTC and CNN-BiLSTM modules produce obvious synergistic effects, and each component can independently reduce prediction error to a certain extent. Compared with WGAN-LSTM and RCATCN-ViT benchmark models, the proposed method shows higher fitting consistency with real life curves and superior comprehensive evaluation scores. For fixture positioning layout multi-objective optimization, this research adopts BPNN to establish an accurate nonlinear mapping between positioning coordinate layout and structural deformation, and introduces dynamic inertia weight improved PSO to solve Pareto optimal solutions with remaining service life, maximum deformation and overall deformation as joint optimization objectives. Taking milling machine fixture as the test object, the BPNN-PSO algorithm converges stably after only 90 iterations with a generation distance of merely 0.011. Under different weight coefficients, the optimized fixture layout achieves smaller structural deformation, and the remaining life ratio peaks at 0.96, obviously outperforming MOGWO-RBF and IPSO-SA contrast algorithms. The integrated scheme realizes coordinated balance of service life and structural stiffness, provides a complete digital design technical path for CNC tool accessories, and possesses great guiding value for actual machining fixture development. Future work will introduce manufacturing cost and assembly

process constraints to further fit practical industrial design demands. In the next research cycle, new datasets of fixture vibration for different types of machine tools such as lathes and drilling machines will be collected to conduct cross machine testing on the CNN BiLSTM life prediction and BPNN-PSO multi-objective optimization model proposed in this paper. By replacing different processing conditions and material samples to verify the generalization ability of the model, comparing the residual life prediction error and structural optimization convergence effect across devices, and comprehensively testing the adaptability and engineering practical value of the entire method in actual processing conditions of multiple types of machine tools.

Acknowledgement

The research is supported by School Grants platform for Scientific Research of Shandong Huayu University of Technology in 2025: CNC tool manufacturing process research and development center PT2025KJX001.

References

[1] Phokobye SN, Desai DA, Tlhabadira RMK. Comparative investigation and optimization of cutting tools performance during milling machining of titanium alloy (Ti6Al4V) using response surface methodology. Int J Adv Manuf Technol. 2024;131(7-8):3565-3577. https://doi.org/10.1007/s00170-024-13225-3

[2] Ageeva EV, Horyakova NM, Sabelnikov BN, Ageeva AE. Optimization of the process of obtaining powder materials for the production of carbide cutting tools by electrodispersion of Tn20 alloy metal waste in water. Proc Southwest State Univ. 2024;28(1):27-43. https://doi.org/10.21869/2223-1560-2024-28-1-27-43

[3] Zhou D, Mei Y, Xu W, Gong H, Suo F. Analysis and optimization of erosion performance of slurry shield cutterhead in high viscosity soil layer. Chin J Undergr Space Eng. 2025;21(4):1344-1351. https://doi.org/10.20174/j.JUSE.2025.04.26

[4] Huo Y, Zhou Y, Liu J, Zhang M, Li Z. A comprehensive cutting tool adaptation method for multi-feature part based on evolutionary game algorithm. Proc Inst Mech Eng Part B J Eng Manuf. 2025;239(8):1078-1091. https://doi.org/10.1177/09544054241260473

[5] Duan C, Cao H, Liu F, Li X, Duan X, Sheng B. Lithium-ion batteries remaining useful life prediction using a parallel BILSTM-MHA neural network based on a CEEMDAN module. Int J Adv Manuf Technol. 2025;137(7):3359-3386. https://doi.org/10.1007/s00170-025-15169-8

[6] Zhang L, Yang Y, Chen Y, Li J, Dai H. Remaining useful life prediction of variable-operating turbofan engine based on VMD-CNN-BiLSTM. J Beijing Univ Aeronaut Astronaut. 2026;52(4):1279-1289. https://doi.org/10.13700/j.bh.1001-5965.2024.0051

[7] Yuan R, Wu F, Li Y, Ou Y. A self-attention health indicator and CNN-BiLSTM based framework for remaining useful life prediction of rolling bearings. J Mech Sci Technol. 2026;40(6):4361-4378. https://doi.org/10.1007/s12206-026-0523-3

[8] Hrechanyi O. Developing an algorithm for planning the periodicity of controls for a random process model. Results Eng. 2024;24:102964. https://doi.org/10.1016/j.rineng.2024.102964

[9] Liu Y, Diao X, Zhu H. Dynamic decoupling control of PMa-BSynRM based on neural network inverse system optimized by enhanced chaos PSO. IEEE Trans Ind Electron. 2025;72(10):9900-9910. https://doi.org/10.1109/TIE.2025.3552268

[10] Lin JF, Sheu JJ. Using PSO and SA for optimizing the retardance in dextran-citrate coated ferrofluids. Neural Comput Appl. 2025;37(2):785-800. https://doi.org/10.1007/s00521-024-10041-4

[11] Belodedenko S, Hrechanyi O, Hanush V, Izhevskyi Y. Experimental and analytical ways of finding the function of the maximum accumulated damage under operating modes with overloads. Adv Ind Manuf Eng. 2024;8:100137. https://doi.org/10.1016/j.aime.2024.100137

[12] Peng C, Chen X, Gao M, Guo J, Guan L, Dai C, et al. A 28 nm dual-mode SRAM-CIM macro with local computing cell for CNNs and grayscale edge detection. IEEE Trans Very Large Scale Integr (VLSI) Syst. 2025;33(8):2264-2273. https://doi.org/10.1109/TVLSI.2025.3578319

[13] Du W, Niu X, Wang H, Gong X, Li A, Li C. A fault diagnosis method for key transmission components of rotating machinery based on SAM-1DCNN-BiLSTM temporal and spatial feature extraction. Proc Inst Mech Eng Part C J Mech Eng Sci. 2025;239(14):5810-5822. https://doi.org/10.1177/09544062251328244

[14] Singh C, Warraich J, Thakkar R, Vo N. SABER: a multimodal sentiment aware regression framework using ROBERTa BiLSTM and deep batch active learning for stock market prediction. Int J Inf Technol. 2025;17(9):5497-5502. https://doi.org/10.1007/s41870-025-02802-8

[15] Sun Q, Wang W, Ren J, Xiong X, Quan L. Aircraft hydraulic system priority valve fault diagnosis research based on WOA-CNN-BiLSTM. IET Conf Proc. 2025;2024(13):1680-1686. https://doi.org/10.1049/icp.2024.3134

[16] Sheyko S, Belokon Y, Hrechanyi O, Vasilchenko T. Thermoplastic processing of structural metallic materials. Cham: Springer; 2024. https://doi.org/10.1007/978-3-031-73896-8
[17] Sheyko S, Tsyganov V, Hrechanyi O, Vasilchenko T, Hrechana AH. Determination of the optimal temperature regime of plastic deformation of micro alloyed automobile wheel steels. Res Eng Struct Mater. 2023;9(4):1305-1318. https://doi.org/10.17515/resm2023.49me0428tn
[18] Krishana BH. Optimized key management scheme based on hashing and PSO algorithm for WSN. IOSR J Comput Eng. 2025;27(2):11-17. https://doi.org/10.9790/0661-2702011117
[19] Zhang L, Liang H, Tang J, Zhang H, Huang Y, Sun H, et al. Research on the precision compensation of light-quantum flowmeter with CPO–PSO–CNN algorithm. IEEE Sensors J. 2025;25(17):33859-33868. https://doi.org/10.1109/JSEN.2025.3591915
[20] Khoudiri A, Khoudiri S, Khaleel M. PSO-enhanced discrete-time integrated sliding mode-based control of three-level NPC converter for grid-connected PV-FC distributed generation system. Stud Eng Exact Sci. 2024;5(1):1028-1056. https://doi.org/10.54021/seesv5n1-054